THREE-PORT DC/DC CONVERTER FOR RENEWABLE ENERGY APPLICATIONS

[1]Mrs.M.Suguna, [2]Mr.P.Velmurugan
[1]Assistant Professor, [2]Assistant Professor
[1]Electrical & Electronics Engineering
[1]Narasu's Sarathy Institute of Technology, Salem, India

Abstract: Integrated three port DC/DC converters are of potential interest in home applications by charging batteries using solar power. An integrated three-port DC/DC converter, which interfaces one solar input port, one bidirectional battery port, and an isolated output port for other use. Compared to the traditional full and half bridge bidirectional DC/DC converters for the similar applications, the new three-port topology has the advantages of simple circuit topology with no Total Device Rating (TDR) penalty, soft-switching implementation without additional devices, high efficiency and simple control. These advantages make the new converter promising for medium and high power applications especially for auxiliary power supply in fuel cell vehicles and power generation where the high power density, low cost, lightweight and high reliability power converters are required. The operating principle, theoretical analysis, and design guidelines are provided in this paper. The simulation and the experimental verifications are also presented with hardware.

Index Terms **– DC/DC converter, TDR.**

I. INTRODUCTION

1.1GENERAL

The increased interest in renewable energy systems with diverse sources has created an unprecedented need for integrated power - electronic converters capable of interfacing, and simultaneously controlling, several power sources. This is important for systems that are capable of harvesting power from solar sources, fuel cells, regenerative braking, and mechanical vibrations used in applications such as communication repeater stations, traffic lights, sensor networks, hybrid-electric vehicles, laptops, and hand-held electronics. Moreover, integrated multiport interface is important since such systems require mass energy storage to compensate for the mismatch between the sourcing and loading power patterns over a regular operating cycle. For example, a solar system, consisting of a regulated load interfaced to a solar array, requires storage batteries for storing excess power and resupplying it to the load when needed. The absence of batteries in such systems results in either wasted energy or large-signal instability and system failure [1]. With a battery installed, maximum power-point tracking (MPPT) can be performed on the solar panel while the load is regulated [2].The mismatch power is handled by the battery by collecting surplus power at light loading and supplying the deficit at heavier loads. To protect the battery, MPPT is disabled and the battery voltage is regulated when the load is light and the battery is fully charged. Such operation will avoid the need for significant over sizing of the solar arrays for a specific application. Utilizing a single power stage to interface and control three power ports, one of which is bidirectional, promises simplified, flexible, cost-effective, and more efficient power harvesting from a variety of power sources.

The integrated multiport converter, instead of several independent converters, has advantages such as less component count and conversion stage because resources like switching devices and storage elements are shared in each switching period. As a result, the integrated system will have a lower overall mass and more compact packaging. In addition, some other advantages of integrated power converters are lower cost, improved reliability, 2 and enhanced dynamic performance due to power stage integration and centralized control. Besides, it requires no communication capabilities that would be necessary for multiple converters. Therefore, the communication delay and error can be avoided with the centralized control structure. Instead of one control input for traditional two-port converter, N-port converter has N-1 control inputs, which requires more modeling effort. Moreover, since the multiport converter has integrated power stage and, thus, multi-input multi-output (MIMO) feature; it necessitates proper decoupling for various control-loops design.

This new three port DC-DC converter is based on a half-bridge topology. Compared to the full-bridge topologies, it has half the component count for the same power rating with no total device rating (TDR) penalty. Therefore, a minimum number of devices is used in the proposed circuit. Also the design has less control and accessory power needs than its full-bridge competitors. All these new features allow efficient power conversion, easy control, and lightweight and compacted packaging. The proposed converter is a good alternative to the conventional converter in high power applications and has distinct advantages for high power density and low cost applications.

II. THREE-PORT DC/DC CONVERTER INTERFACE

2.1 CIRCUIT EXPLANATION

The basic concept enabling single-stage three-port interface is the striking similarity between the half-bridge and the active-clamp forward converter topologies. As shown in Fig. 2.1, the half-bridge and active-clamp forward are the same with the primary source connected to different points. Adding a free-wheeling branch across the transformer, consisting of a diode and a switch, yields the proposed three-port topology, as shown in Fig.1.1. Its basic steady-state switching waveforms are shown in Fig. 2.2. It is notable that the proposed converter is topologically similar to the zero-voltage-switched (ZVS) duty-cycle shift controlled symmetric half-bridge (DCS–HB) converter reported in [9]. The fundamental difference is that the DCS–HB topology is a two-port topology with its two main switches, S1 and S2, operated at equal duty cycles. The proposed three-port topology independently controls the duty cycles of these switches in order to introduce an additional control variable necessary for interfacing the added bidirectional port. This modification results in asymmetric operation of the topology and changes the design constraints on the converter components, while preserving the topological ability for ZVS.

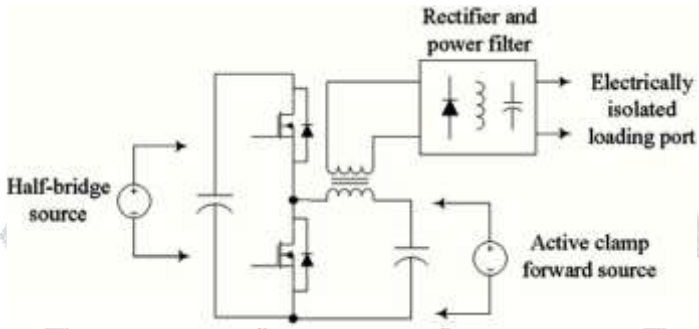

Fig.2.1. Equivalence of the half-bridge and active-clamp forward converter topologies.

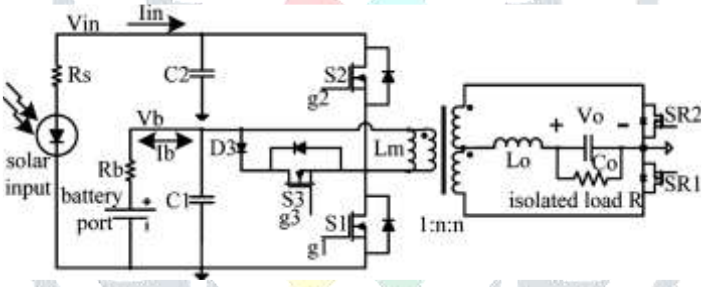

Fig.2.2. Three-port modified half-bridge converter topology

2.2 PRINCIPLE OF OPERATION

This section introduces the three-port topology and control structure. As shown in Fig. 2.2, it is a modified version of pulse width-modulated (PWM) half-bridge converter that includes three basic circuit stages within a constant-frequency switching cycle to provide two independent control variables, namely, duty-cycles d1 and d2 that are used to control S1 and S2, respectively. This allows tight control over two of the converter ports, while the third port provides the power balance in the system. The switching sequence ensures a clamping path for the energy of the leakage inductance of the transformer at all times. This energy is further utilized to achieve ZVS for all primary switches for a wide range of source and load conditions.

2.3 OPERATIONAL STAGES

Having different operational modes is one of the unique features for three-port converters. As illustrated in Fig.2.2. Since MPPT can notably boost solar energy extraction of a photovoltaic (PV) system, the longer insolation period means that MPPT is more often operated to allow a smaller solar array while managing the same amount of load. Two assumptions are made to simplify the analysis: 1) load power is assumed to be constant and 2) battery over discharge is ignored because PV arrays and batteries are typically oversized.

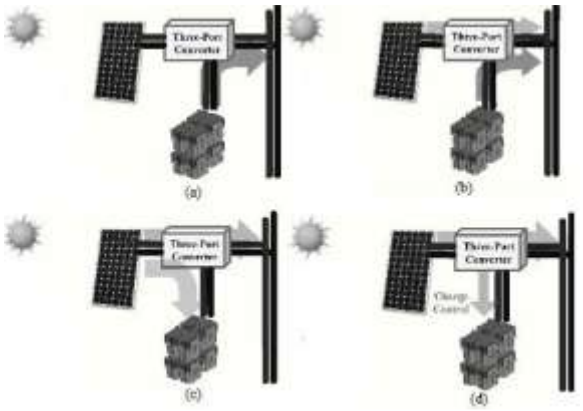

Fig.2.3. Different stages of operation

Fig.2.3showsthe operational modes. Three-port converter can achieve MPPT, battery charge control, and load regulation depending on available solar power, battery state of charge, and load profile. In stage I, battery acts as the exclusive source during eclipse period. In stages II and III, solar power is maximized to decrease battery state of discharge in stage II for initial insolation period, and then to increase battery state of charge in stage III for increased insolation period. In stage IV, battery charge control is applied to prevent battery overcharging and extend battery service life. (a) Stage I operation (eclipse period). (b) Stage II operation (initial insolation). (c) Stage III operation (increased insolation). (d) Stage IV operation (battery charge control).

III.MODELLING AND CONTROL DESIGN

3.1 CONTROL STRUCTURE

The multi-objective control architecture that aims to regulate different power ports are shown in Fig. 3.1, control loops has a PIC microcontroller. The output-port loop is simply a voltage-mode control loop, closed around the load voltage, battery voltage Vbis almost constant and transformer turn's ratio n is fixed. As a result, PIC is assigned to control either input port or battery port.

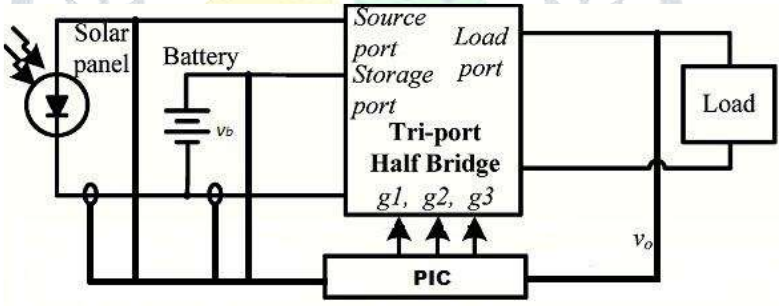

Fig.3.1. Three-port converter's control architecture

State equation for the different stages is derived to get small-signal model which is the basis for optimized controller design. Especially for such a complicated MIMO system of three-port converter, an effective model will be helpful to realize closed-loop control, and furthermore, to optimize the converter dynamics. Since there are two modes of operation f or the three-port converter, small-signal models in both modes need to be obtained separately. Unlike conventional two-port converter, multiport converter is a high-order system, and the symbolic derivation of these plant transfer functions is fairly tedious; therefore, it is difficult to obtain values of poles and zeros for analysis. A common problem about MIMO system is the existence of various interacting control loops that complicate compensator designs; therefore, a controller like PIC is introduced to allow separate controller designs for each of the three power port.

3.2 MODELLING DURING BATTERY-REGULATION MODE

Before deriving for small-signal transfer functions of the converter, state equations for four energy storage elements during each circuit stage are developed. For battery-regulation mode, these include the battery capacitor C1, the transformer magnetizing inductance Lm, the output inductance Lo, and the output capacitance Co. There are three main circuit stages, as illustrated in Fig.3.2.The battery-regulation mode consists of three stages as shown in the waveform timing diagramFig.3.2. The stages are classified based on the gating pulse to the respective gates of the switch used here say MOSFET (Metal Oxide Semiconductor Field Effect Transistor). The waveform timing diagram is plotted for the gating pulses, primary transformer

voltage given as Vpri, output inductor current represented by the symbol ILo. Here MOSFET is used as the switching device because of its high switching speed compared to the other devices, this can be easily turned-on and turned-off and is often used as a pilot gate device for thyristor. The voltage rating for this is around 1000V and also current rating is around 100A.

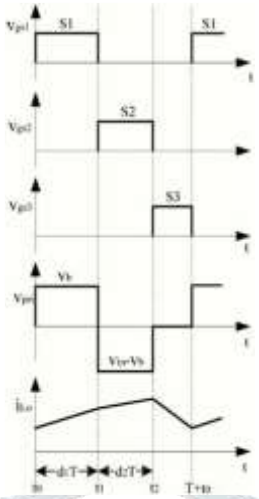

Fig.3.2 Basic Gate Pulse waveforms for three-port

Where, converter variables Vpri and ILo represent transformer primary-side voltage and output inductor current, respectively as represented in the above figure.10From above timing diagram waveform for the gate of the MOSFET, primary transform voltage and current of output inductor are given. The following are three stages as shown in Fig.3.2.as follows:
Stage I (t0-t1)
Stage II (t1-t2)
Stage III (t2-t3)
after this three stages again there is repetition of the same cycle takes place.

STAGE I (t0-t1):

Stage I (t0-t1): In stage I, S1 is gated ON, applying a positive voltage to the transformer primary side, while output inductor is charging. Synchronous Switch SR1 is gated ON to allow current flow through output inductor Lo. Current ofbattery-port filter capacitor is equal to the s um of battery current, transformer magnetizing inductor current, and reflected secondary-side current. The state equation in this stage is as follows:
C1dvc1/dt = –vc1/Rb + iLm –niLo(3.1)
LmdiLm/dt = –vc1(3.2)
LodiLm/dt = vc1n –vo(3.3)
Codvo/dt = iLo–vo/R(3.4)

Stage II (t 1–t 2):

Stage II (t 1–t 2): In stage II, S2 is gated ON, a negative voltage is applied to the transformer primary side, and output inductor is still charging. Synchronous switch SR2 is gated ON to allow a current flow path through Lo. The transformer primary voltage is the input voltage that subtracts battery voltage, and thus, output inductor charging rate changes accordingly. The state equationin this stage is as follows:
C1dvc1/dt = –vc1/Rb + iLm + niLo(3.5)
LmdiLm/dt = –vc2–vc1(3.6)
LodiLm/dt = (vc2 –vc1)n –vo(3.7)
Codvo/dt = iLo –vo/R(3.8)

Stage III (t 2–T+t0):

Stage III (t 2–T+t0): In stage III, S3 i s gated ON, zero voltage is applied to the transformer primary side due to middle branch(S3 and D3 path)'s clamping, and output inductor is discharging. This allows both the magnetizing and output inductor currents to free-wheel. Both SR1 and SR2 are turned on, thus output inductor current distributes into both of rectifying paths. The state equation in this stage is as follows:
C1dvc1/dt = –vc1/Rb(3.9)
LmdiLm/dt = 0(3.10)
LodiLm/dt = –vo(3.11)
Codvo/dt = iLo –vo/R(3.12)
the above three stages and there corresponding state equation represents the current flow. The model graph shown in Fig.3.2 Basic Gate Pulse waveforms for three-port and also the transformers primary-side voltage and output inductor current. These

stages are repeated, while we get a DC current in the output. The model graph is verified using Matlab software. SIMULINK tool is used for simulation and results are given in following chapters. Hardware implementation of this three-port DC-DC converter is also done.

IV.HARDWARE IMPLEMENTATION OF CONTROL CIRCUIT

4.1ORGANISATION OF CONTROL CIRCUIT

The control circuit employs the following blocks. These are explained in the forthcoming topics

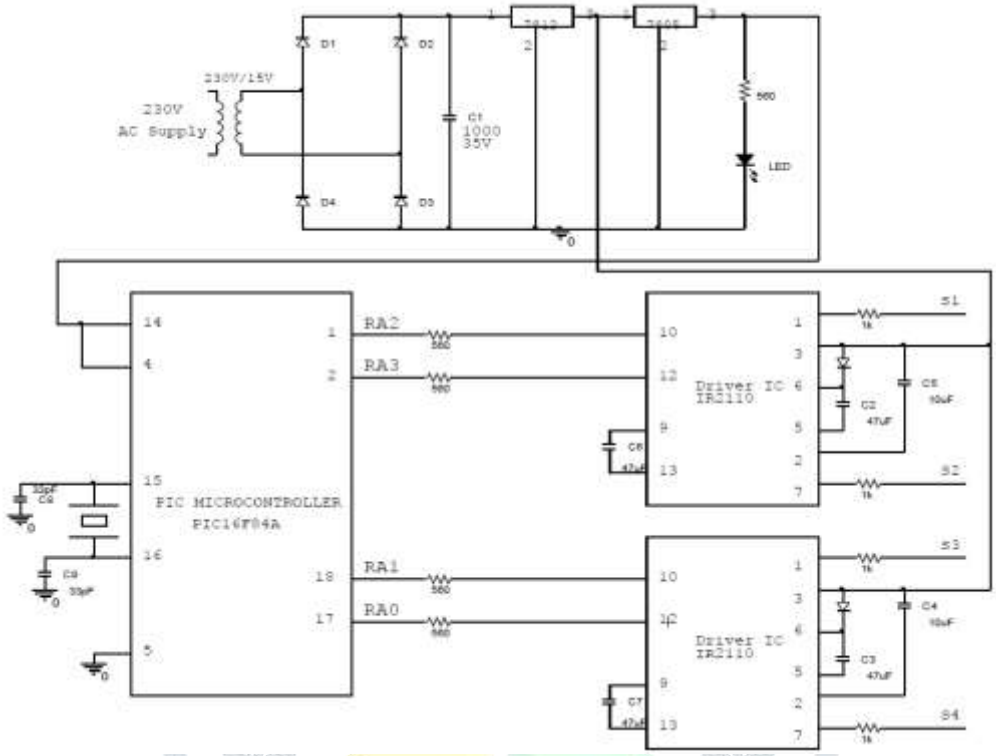

Fig.4.1Block Diagram of Control Circuit

For the hardware implementation we use different components. They are listed below as

- PIC Microcontroller 16F84A.
- Voltage Regulators
  a.7812 voltage regulator
  b.7805 voltage regulator
- IC IRS2110 for the amplification of the pulses given
- by PIC16F84A
- Power MOSFET as switching device IRF840

V.SIMULATION RESULTS

5.1 CIRUIT PARAMETERS

Various elements used for designing the circuit are:

- Output Inductor L_o
- Magnetizing Inductor L_m
- Output filter Capacitor C_o
- Battery port filter Capacitor C_1
- Output voltage V_o
- Input Voltage $V_{in}(V_{c2})$
- Battery Voltage $V_b(V_{c1})$

- Input port filter Capacitor C_2

5.2 CONVENTIONAL CIRCUIT DIAGRAM

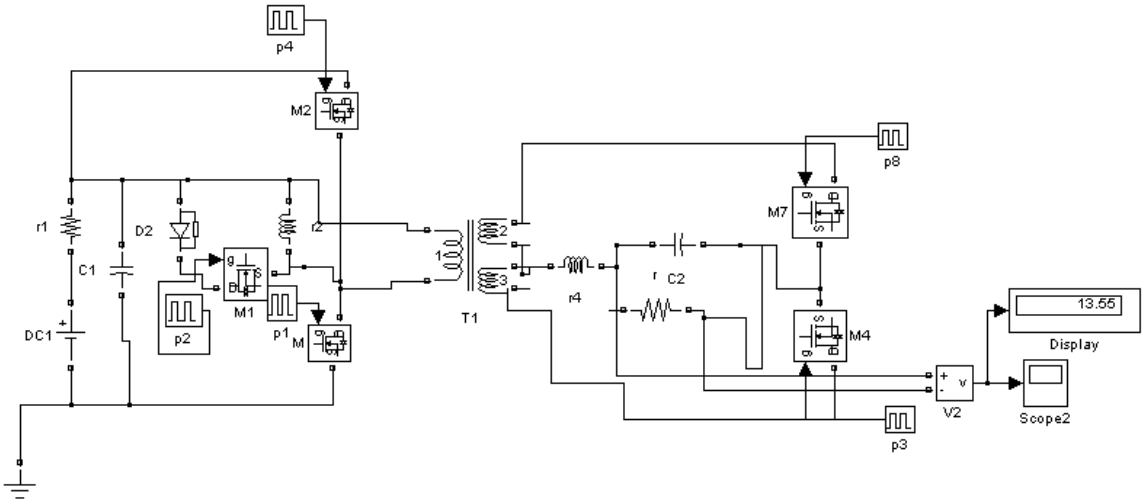

Fig.5.1. Conventional circuit diagram

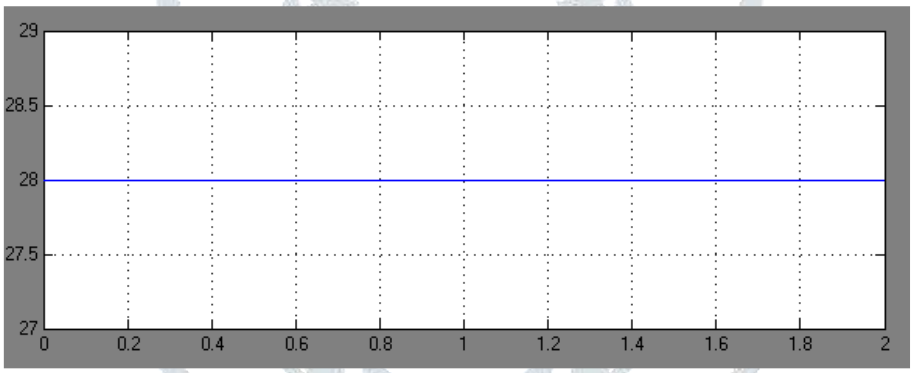

Fig.5.2. Dc input voltage

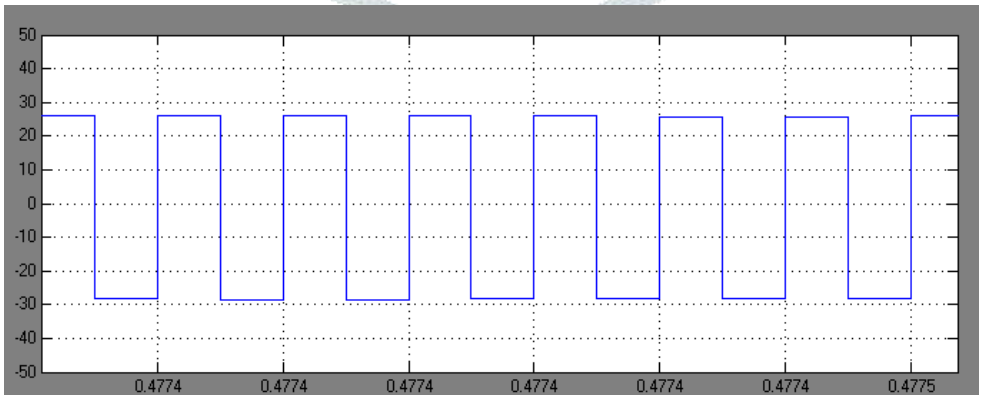

Fig.5.3. Transformer secondary voltage

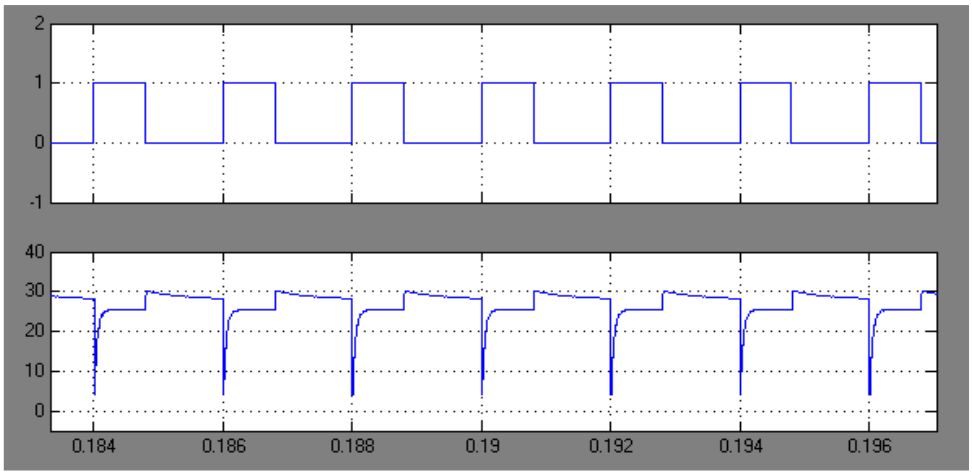

Fig.5.4. Gate pulse MOSFET (M) And voltage across the drain to source voltage(V_{ds})

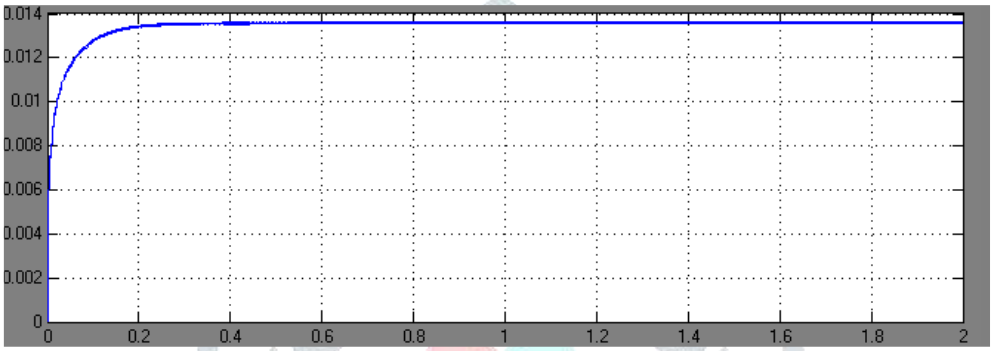

Fig.5.5. Output current wave form

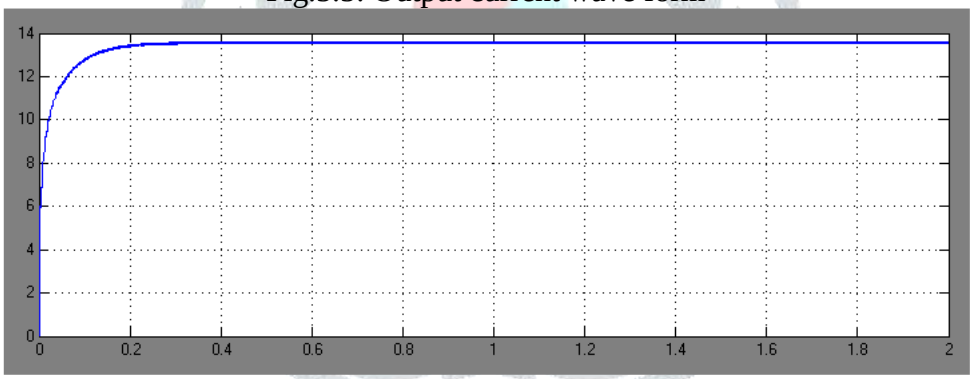

Fig.5.6. Output voltage waveform

5.3 PROPOSED CIRCUIT DIAGRAM

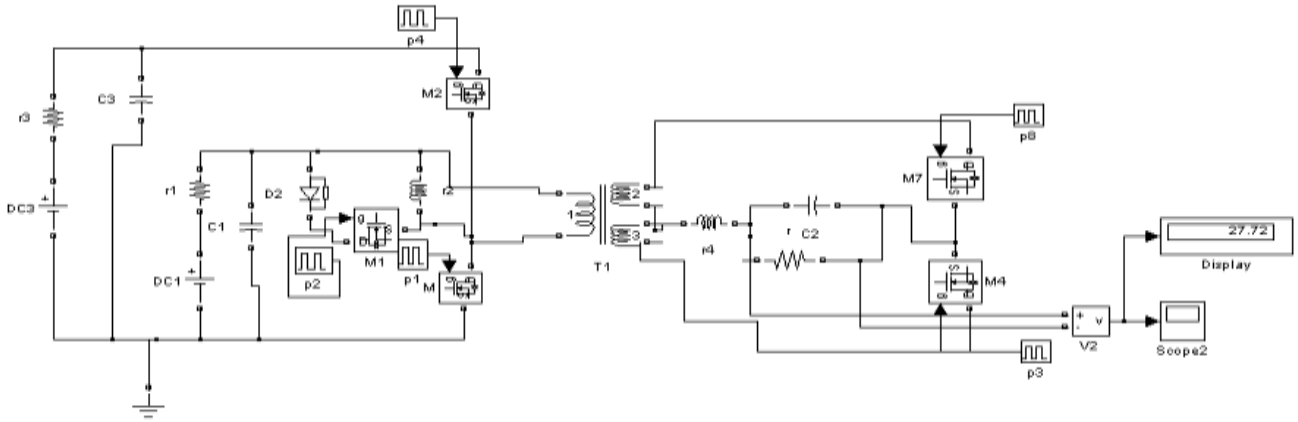

Fig.5.7. Three port circuit diagram

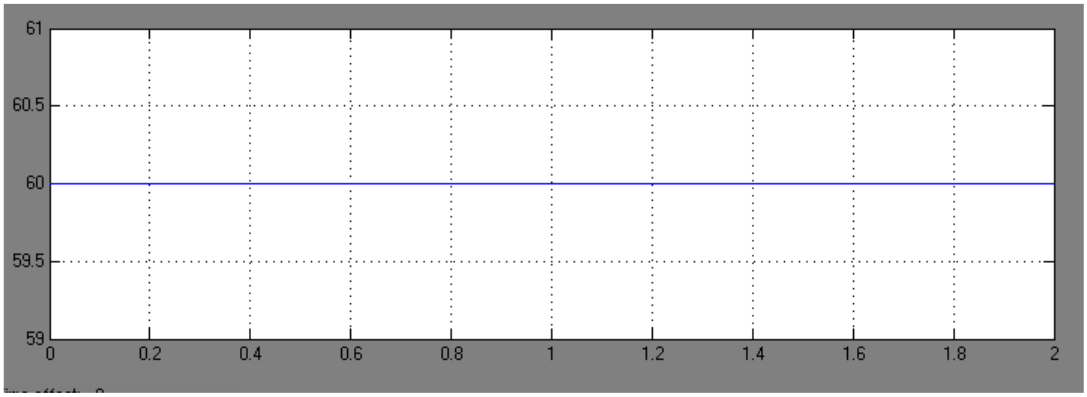

Fig.5.8. Solar input voltage

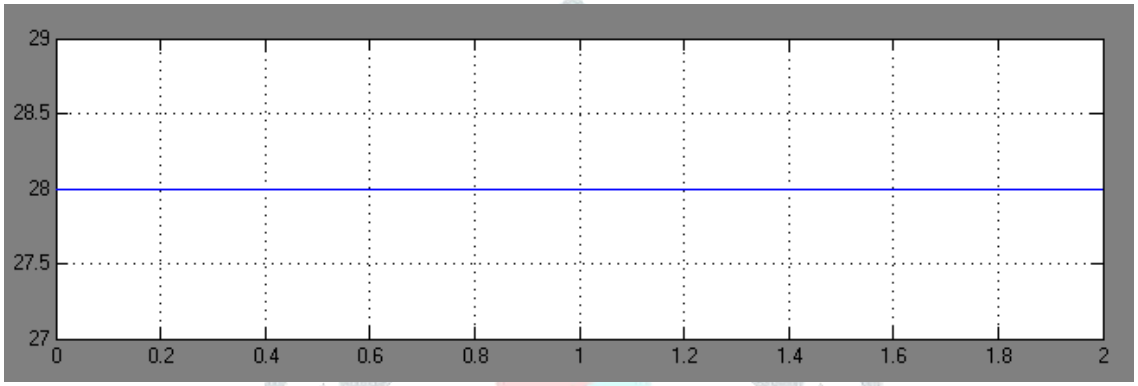

Fig.5.9. Dc battery input voltage

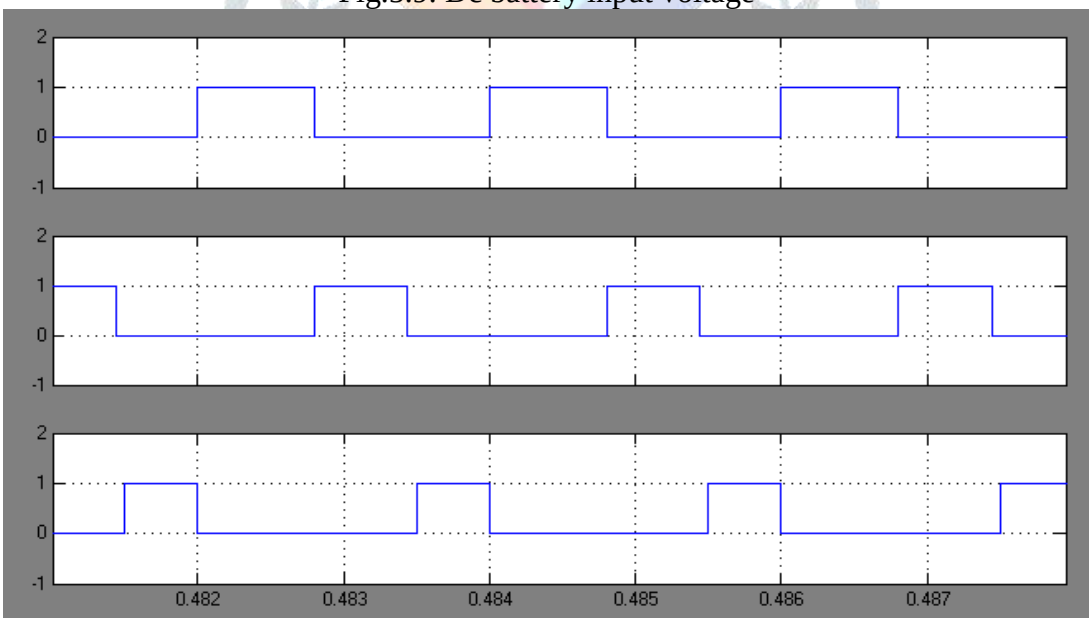

Fig.5.10. Gate pulse (M, M1, M2)

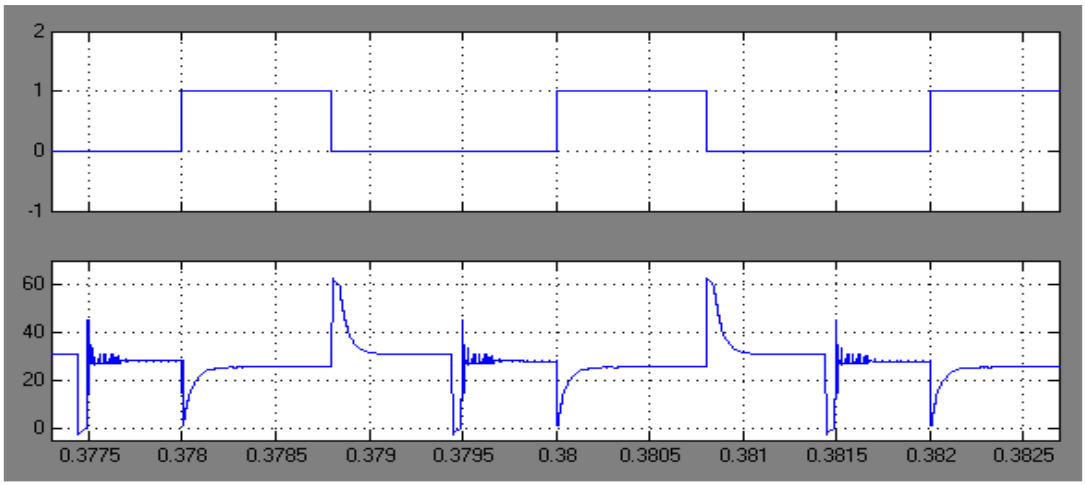

Fig.5.11. M2 gate pulse and voltage across M2 (V_{ds})

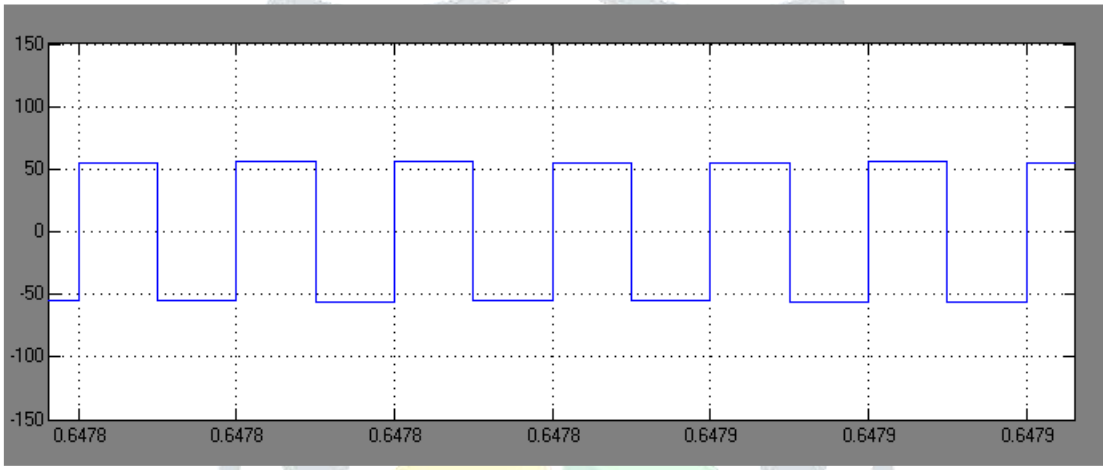

Fig.5.12. Voltage across transformer secondary voltage

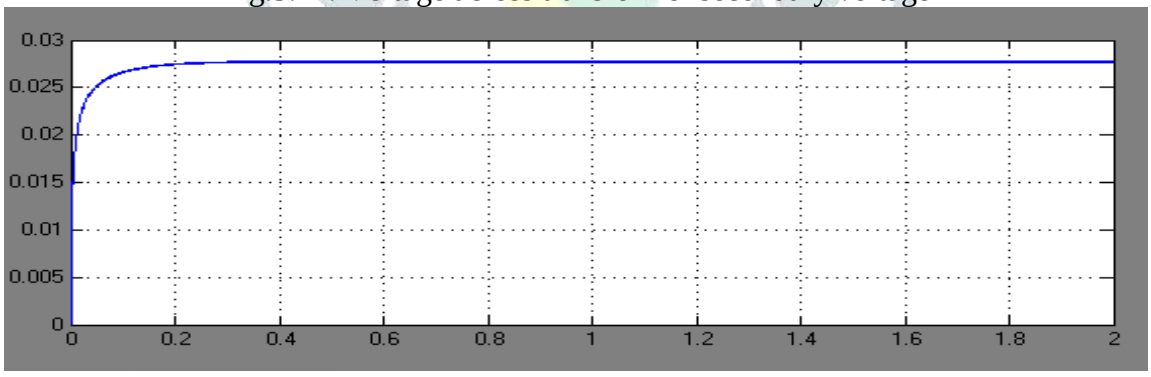

Fig.5.13. Output current waveform

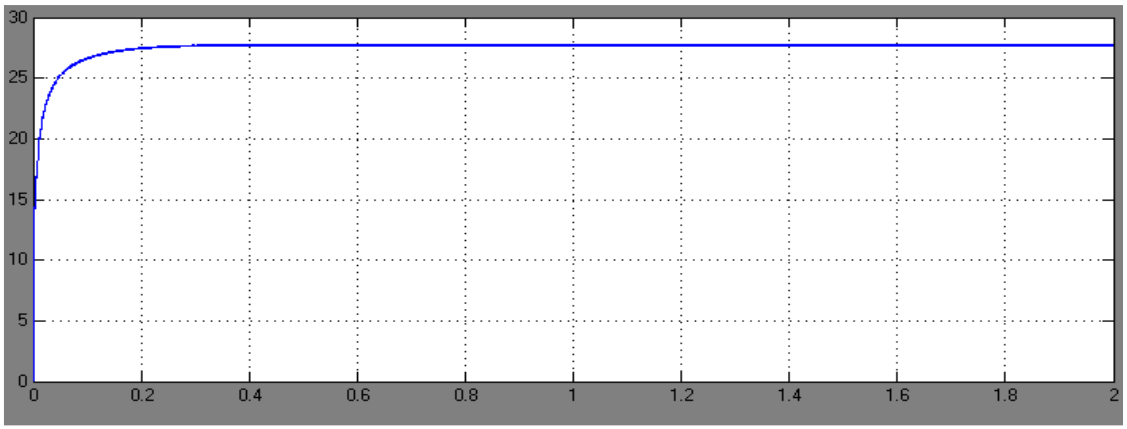

Fig.5.14. Output voltage waveform

CONCLUSION

Presented three-port DC/DC converter topology capable of interfacing three dc power ports: a primary source, bidirectional storage, and an isolated load. This converter is suitable for renewable energy systems where bulk energy storage is required. Among other applications, it is valuable for bundling batteries with solar arrays, or super-capacitors with fuel cells, while allowing tight load regulation. Simulation and experimental results were shown to verify the operation principle, which is more reliable than the conventional converters. However hardware implementation of this converter is not up to mark as the simulation results, it requires large solar panel which is more cost and large batteries to store the power generated, also increased the overall cost. Also by using Maximum Power Point Tracking (MPPT), with this three-port DC/DC converter to yield more power.

REFERENCES

[1]A. Emadi, J. P. Johnson, and M. Ehsani,(2000)"Stability analysis of large DC solid-state power systems for space," IEEE Aerosp. Electron.Syst.
[2] A. Capel,(1998)"The power system of the multimedia constellation satellite for the SKYBRIDGE missions," in Proc. IEEE Power Electron. Spec.Conf.
[3] A. Di Napoli, F. Crescimbini, L. Solero, F. Caricchi, and F. G. Capponi,(2002)"Multiple-input DC–DC power converter for power-
flow management in hybrid vehicles," in Proc. IEEE Ind. Appl. Conf.
[4]B. G. Dobbs and P. L. Chapman,(2003)"A multiple-input DC–DC converter topology," IEEE Power Electron.
[5] D. Liu and H. Li,(2006)"A ZVS bi-directional DC–DC converter for multiple energy storage elements," IEEE Trans. Power Electron.
[6] F. D. Rodriguez and W. G. Imes,(1994)"Analysis and modeling of a two-input DC/DC converter with two controlled variables and four switched networks," in Proc. AIAA Int. Energy Convers. Eng. Conf.
[7] G.-J. Su and F. Z. Peng,(2005)"A low cost, triple-voltage bus DC
–DC converter for automotive applications," in Proc. IEEE Appl. Power Electron.Conf.
[8] H. Al-Atrash, F. Tian, and I. Batarseh,(2007)"Tri-modal half-bridge converter topology for three-port interface," IEEE Trans. Power Electron.
[9]H. Mao, J. Abu-Qahouq, S. Luo, and I. Batarseh,(2004)"Zero-voltage-switching half-bridge dc–dc converter with modified PWM controlmethod," IEEE Trans. Power Electron.
[10] W. G. Imes and F. D. Rodriguez,(1994) "A two-input tri-state converter for spacecraft power conditioning," in Proc. AIAA Int. Energy Convers. Eng. Conf.